

Electronic Supplementary Information (ESI)

Incorporation of sulfur vacancies in ZnIn₂S₄ photoanode for highly efficient photoelectrochemical water splitting and urea oxidation

Peiyue Hu, Chuanyi Ruan, Jingjing Quan, Chenglong Li, Xingming Ning*, Pei Chen*, Zhongwei An and Xinbing Chen*

Key Laboratory of Applied Surface and Colloid Chemistry (MOE), Shaanxi Key Laboratory for Advanced Energy Devices, Shaanxi Engineering Laboratory for Advanced Energy Technology, International Joint Research Center of Shaanxi Province for Photoelectric Materials Science. School of Materials Science and Engineering, Shaanxi Normal University, Xi'an, 710119, PR China.

**Corresponding author, E-mail: ningxingming@snnu.edu.cn, chenpei@snnu.edu.cn, chenxinbing@snnu.edu.cn*

TABLE OF CONTENTS

S 1. Experimental Section	3
S 1.1 Materials and Reagents	3
S 1.2 Physical Measurements and Instruments	3
S 1.3 Electrochemical Measurements	3
S 1.4 Photoelectrochemical Measurements	4
S 2. Preparation Details	5
S 3. Additional Figures and Discussions	7
S 3.1 Experimental Data	7
S 3.2 Reference	18

S 1. Experimental Section

S 1.1 Materials and Reagents

Zinc chloride (ZnCl_2 , 98.00%), Indium trichloride tetrahydrate ($\text{InCl}_3 \cdot 4\text{H}_2\text{O}$, 98.00%), Thiourea ($\text{C}_7\text{H}_8\text{N}_2\text{S}$, 99.00%) were selected from Shanghai Maclin Biochemical Technology Co., LTD. Absolute ethanol ($\text{C}_2\text{H}_6\text{O}$), and Acetone ($\text{C}_3\text{H}_6\text{O}$, $\geq 99.50\%$), Disodium hydrogen phosphate dodecahydrate ($\text{Na}_2\text{HPO}_4 \cdot 12\text{H}_2\text{O}$, AR), Sodium dihydrogen phosphate dihydrate ($\text{NaH}_2\text{PO}_4 \cdot 2\text{H}_2\text{O}$, AR), Anhydrous sodium sulfite (Na_2SO_3 , AR), Nitric acid (HNO_3 , AR), Potassium chloride (KCl , $\geq 99.50\%$) were obtained from Sinopharm Chemical Reagent Co., Ltd. Potassium ferrocyanide trihydrate ($\text{K}_4[\text{Fe}(\text{CN})_6] \cdot 3\text{H}_2\text{O}$, $\geq 99.00\%$), Potassium ferricyanide ($\text{K}_3[\text{Fe}(\text{CN})_6]$, $\geq 99.50\%$) were purchased from Shanghai Aladdin Biochemical Technology Co., Ltd. Fluorine-doped SnO_2 (FTO, 14Ω per square) glasses were achieved from Wuhan Jinge Solar Energy Technology Co., Ltd.

S 1.2 Physical Measurements and Instruments

The morphology of the different photoanodes was explored by emission scanning electron microscope (SEM, SU8020). Transmission electron microscopy (TEM) and high-resolution TEM (HR-TEM) images were carried out using a JEM2100 (200 kV). The chemical state and composition were investigated by X-ray photoelectron spectroscopy (XPS, Escalab Xi⁺). The crystal structure of the sample was characterized by X-ray diffraction (XRD, Shimadzu XRD-6000 diffractometer), and the light absorption capacity of the sample was determined by ultraviolet visible near-infrared spectrometer (Shimadzu UV-3600). The structure was measured by fourier transform microinfrared spectroscopy (FTIR, Bruker, Tensor27). The contact angle (KRUSS-DSA100, Germany) was used to test the affinity of the sample surface and analyze the surface properties of the sample. Time-resolved photoluminescence (TRPL) spectroscopy was measured on Fluorolog-QM (HORIBA). Sulfur vacancies was tested by electron paramagnetic resonance (EPR, EMX-10/12).

S 1.3 Electrochemical Measurements

Electrochemical tests were carried out on CHI760E, thereinto fluorine-doped tin oxide glass with different samples as working electrode. Cyclic voltammogram (CV) curves were obtained with different scan rates, such as 150 mV/s and 100 mV/s. Oxygen evolution reaction (OER) measurements were performed on a standard three-electrode system in dark conditions.

S 1.4 Photoelectrochemical (PEC) Measurements

The PEC test was carried out through an electrochemical workstation (CHI760), including a traditional three-electrode system with a scan rate of 50 mV/s. Where the prepared ZIS, ZIS-SV-2h and ZIS-SV-4h photoanodes were used as working electrodes, the saturated Ag/AgCl electrode was used as reference electrode, the Pt plate electrode was used as counter electrode, and the electrolyte was 0.5 M Na₂HPO₄/NaH₂PO₄ buffer solution (PBS, pH 6.5). Thereinto, 300 W Xenon arc lamp (Beijing Perfectlight Technology Co. Ltd., PLS-SXE300D) equipped with a filter (AM 1.5 G), was viewed as a simulated solar illumination AM 1.5 G (100 mW/cm²). The current-time (*I-t*) curves of ZIS and ZIS-SV-2h photoanodes were carried out at 1.0 V_{RHE}.

The electrochemical impedance spectroscopy (EIS) was measured at 0 V versus Ag/AgCl in 0.5 M PBS (10 KHz to 0.1 Hz). Where R_{ct} is charge transfer resistance, R_s is the solution resistance, and CPE is the constant phase angle, respectively.

The applied bias photon-current efficiency (ABPE) is calculated as follows¹:

$$ABPE(\%) = \frac{J \times (1.23 - V_b)}{P_{light}} \times 100 \%$$

Where J is the photocurrent density (mA/cm²), V_b is the applied voltage, and P_{light} is the light intensity (100 mW/cm²).

The surface charge separation efficiency of the photoanode is calculated using the following equation¹:

$$\eta_{sep}(\%) = \frac{J_{H_2O}}{J_{Na_2SO_3}} \times 100\%$$

Where J_{H_2O} and $J_{Na_2SO_3}$ is the photocurrent density achieved in a 0.5 M PBS electrolyte without or with Na_2SO_3 , respectively.

The potential can be converted to a reversible hydrogen electrode (RHE, E_{RHE}) by Nernst equation¹:

$$E_{RHE} = E^0_{Ag/AgCl} + 0.197 + 0.0591 \text{ pH}$$

Where the value of $E^0_{Ag/AgCl}$ is 0.1976 V at 25 °C.

The intensity modulated photocurrent spectroscopy (IMPS) was tested using photochem system (LED, 470 nm) of Autolab M204. The IMPS plots were measured over a frequency range from 10 KHz to 0.1 Hz in 0.5 M PBS solution. And the $I-t$ curves were recorded at the same potential with IMPS by using a light source (LED, 470 nm). The average lifetime (τ) can be gained by the following formula¹:

$$\tau_d = \frac{1}{2\pi f_{IMPS}}$$

Where f_{IMPS} is the frequency, which is located of the lowest point in the IMPS plot.

S 2. Preparation Details

Preparation of nanosheets $ZnIn_2S_4$ (ZIS): ZIS nanosheets were prepared by a hydrothermal method. Firstly, 0.0545 g $ZnCl_2$, 0.1759 g $InCl_3 \cdot 4H_2O$, and 0.1217 g CH_4N_2S were dissolved in 40 mL deionized water to obtained precursor solution. Then, fluorine-doped tin oxide glass (FTO) was placed into the autoclave with 10 mL precursor solution. It is should be noted that the FTO leaned against the wall of the autoclave, and the conductive side was downward. Where the temperature and time were set to 160 °C and 7 h respectively. Finally, the expected ZIS based photoanodes were washed with DI water and absolute ethanol for 3 times.

Preparation of ZnIn₂S₄-Sulfur vacancies (ZIS-Sv) photoanodes: The ZIS-Sv photoanodes were obtained by a simple annealing process through a muffle furnace (5 °C/min) for different temperatures (230 °C, 250 °C and 280 °C) for 1 h. Afterwards, the annealing temperature was optimized by linear sweep voltammetry curves. Where the optimal temperature is 250, which was selected to prepare the ZIS photoanode with Sv (named as ZIS-Sv). Finally, the ZIS-Sv-xh (where x = 0h, 2h, and 4h) could also be achieved through a simple annealing process (250 °C) in a muffle furnace for different times (0h, 2h, and 4h).

S 3. Additional Figures and Discussions

S 3.1 Experimental Data

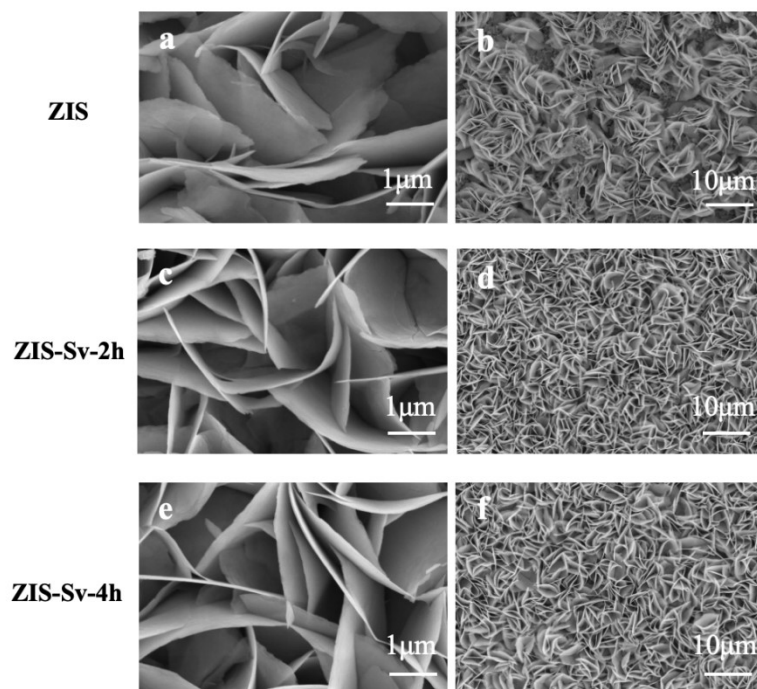


Fig. S1 Scanning electron microscopy images of ZIS, ZIS-Sv-2h and ZIS-Sv-4h.

According to Fig. S1, ZIS, ZIS-Sv-2h, and ZIS-Sv-4h photoanodes exhibit similar structures, suggesting that the incorporation of Sv through heat treatment does not alter the morphology of ZIS.

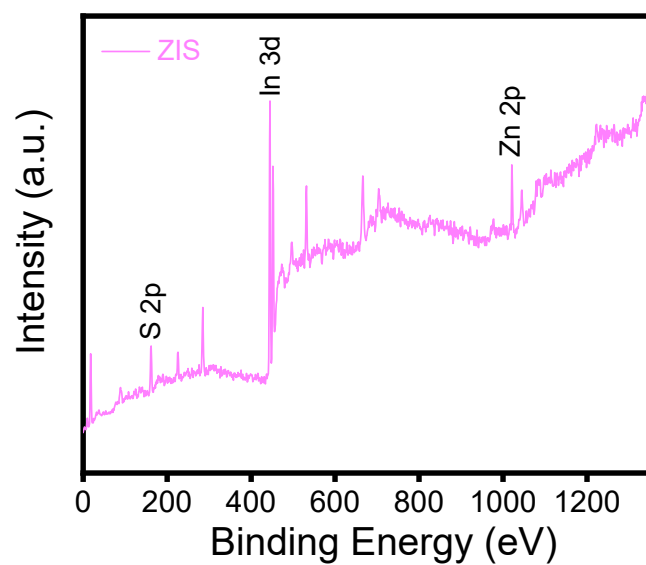


Fig. S2 XPS survey spectra of ZIS.

XPS survey spectra prove the existence of Zn, In, and S elements.

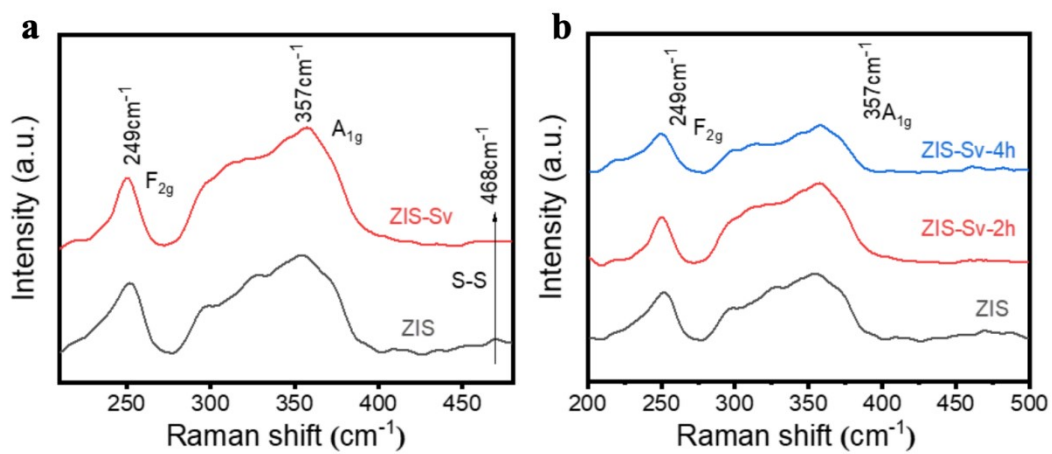


Fig. S3 Raman spectra of different samples.

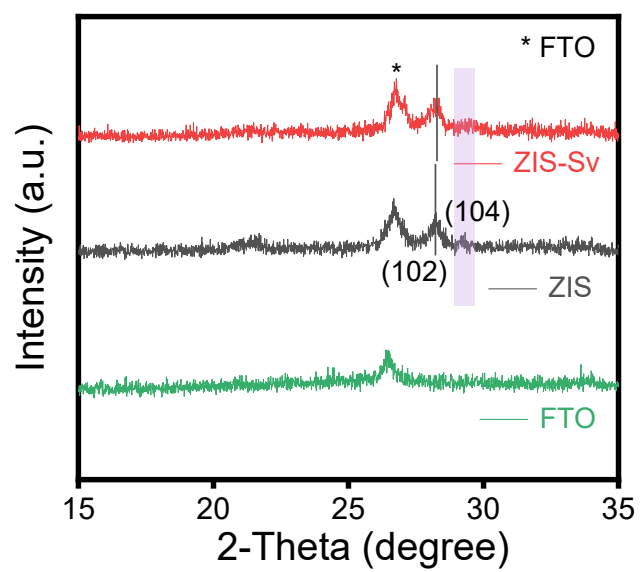


Fig. S4 XRD patterns of FTO, ZIS and ZIS-Sv.

In the Fig. S4, the shift of XRD peak position indicates the presence of Sv in ZIS photoanode.

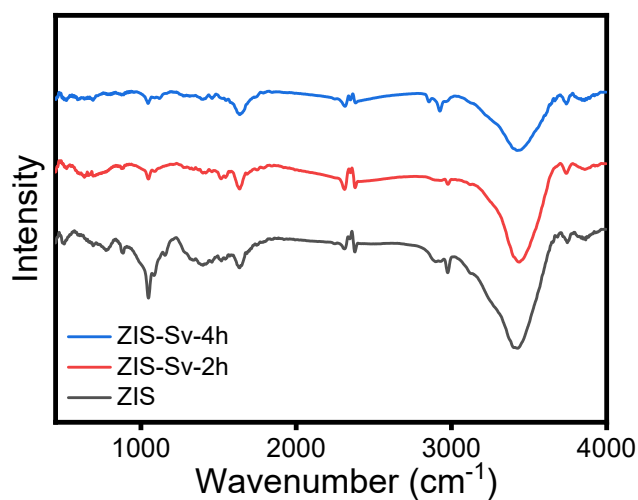


Fig. S5 Fourier transform infrared (FT-IR) spectra of different photoanodes.

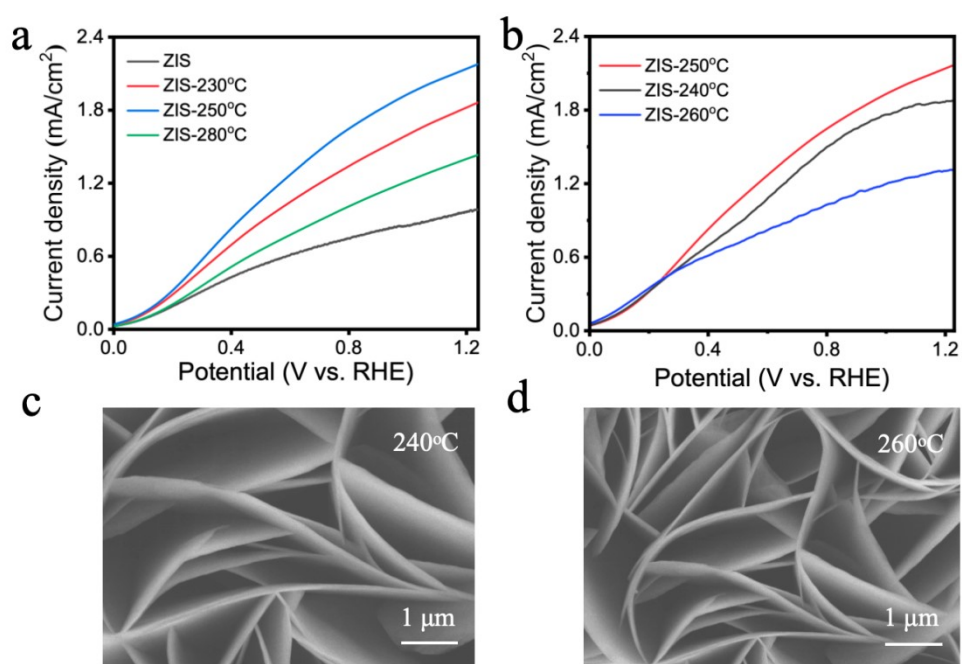


Fig. S6 (a,b) Photocurrent densities of ZIS based photoanodes at different temperatures. (c,d) SEM images of ZIS based photoanodes at different temperatures.

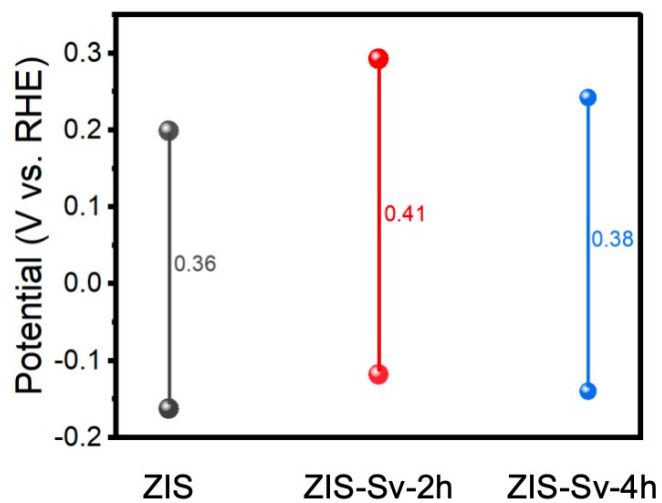


Fig. S7 The open-circuit potential (OCP) values under both dark and light conditions.

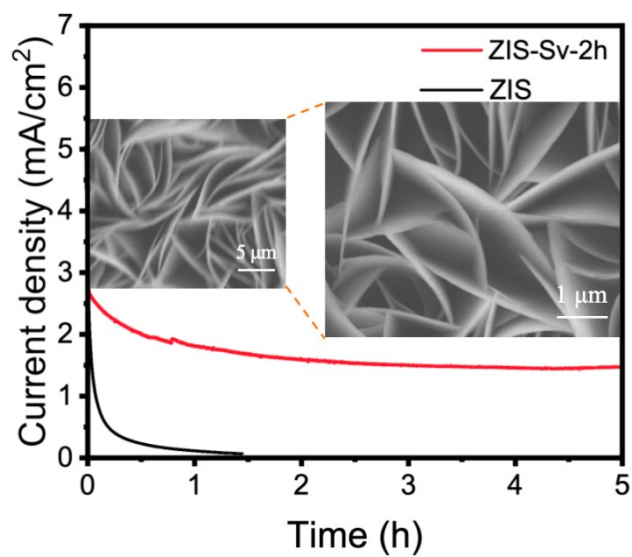


Fig. S8 *I-t* curves of ZIS and ZIS-Sv-2h photoanodes (insets show the SEM images of ZIS-Sv-2h after PEC tests).

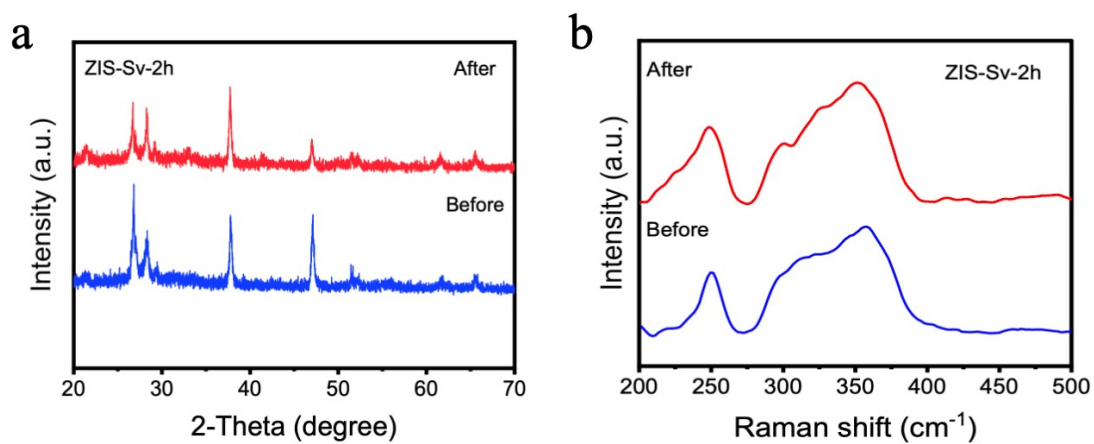


Fig. S9 (a) XRD of ZIS-Sv-2h before and after PEC tests, respectively. (b) Raman spectra of ZIS-Sv-2h before and after PEC tests, respectively.

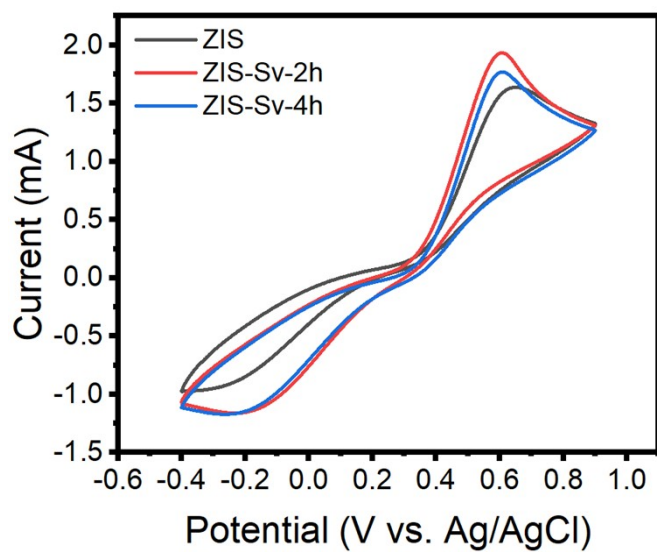


Fig. S10 Cyclic voltammograms (CVs) for different samples (50 mV/s).

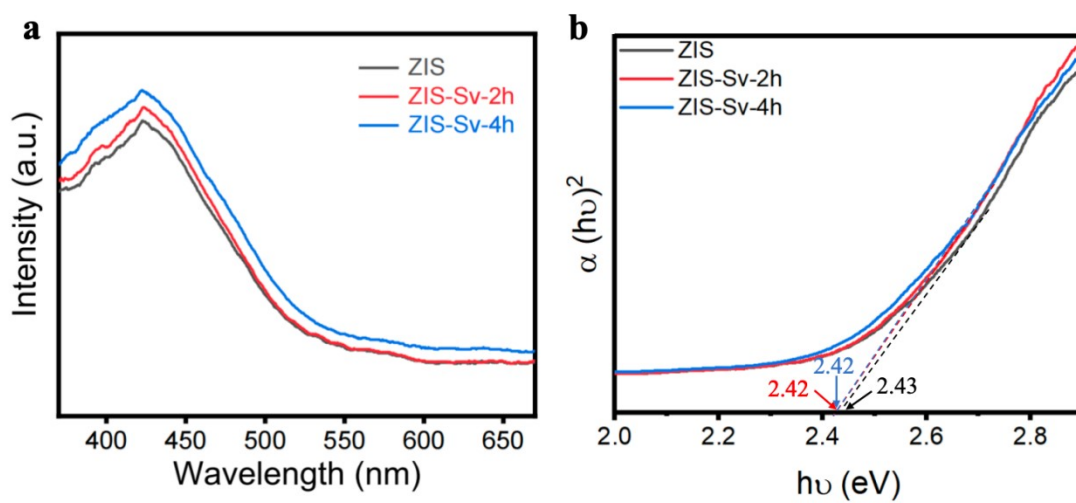


Fig. S11 Diffuse reflectance spectroscopy (DRS) and Tauc plots of different samples.

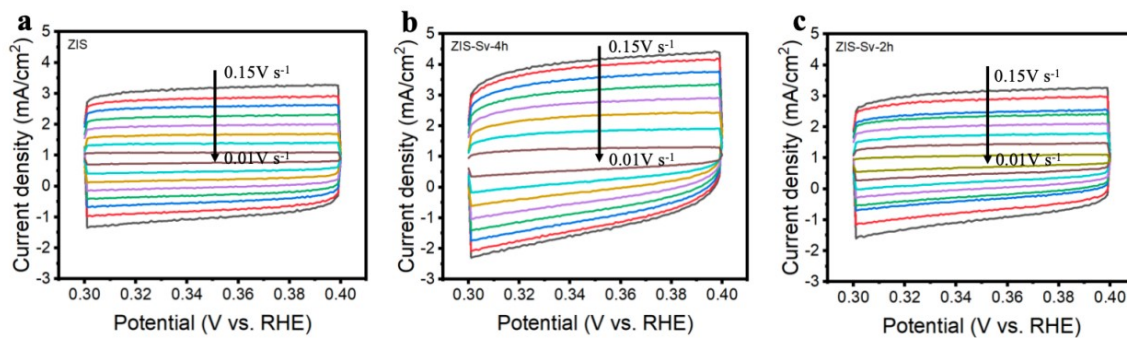


Fig. S12 CVs of different samples with different scan rates.

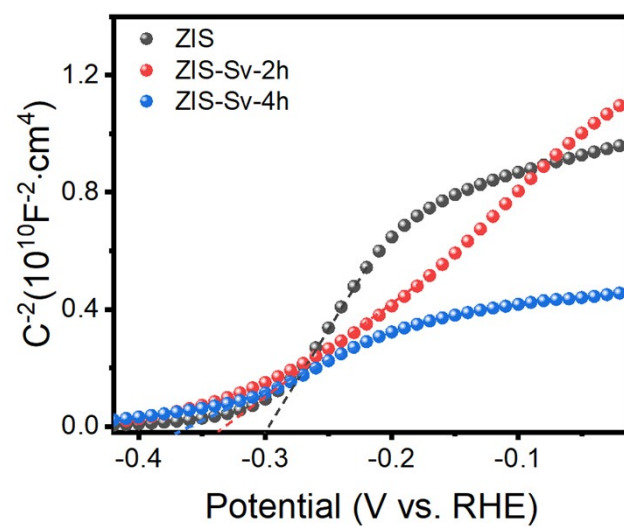


Fig. S13 Mott-Schottky (M-S) plots of different samples.

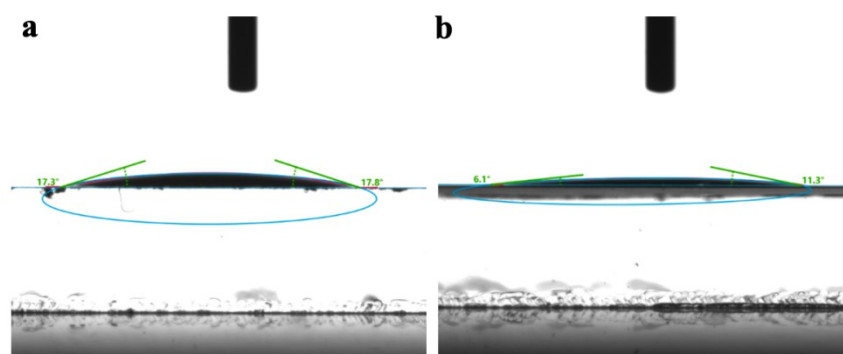


Fig. S14 Contact angle on (a) ZIS and (b) ZIS-Sv-4h

Table S1. Summary of recent significant progress of ZIS-based photoanodes.

Photoanodes	Photocurrent		Journal	Year	Ref
	at 1.23 V vs. RHE				
Co-Pi/ZnIn ₂ S ₄ /Pt	0.91 mA/cm ²		<i>Appl. Catal., B Environ.</i>	2019	2
ZnIn ₂ S ₄ /CdS	1.35 mA/cm ²		<i>Adv. Energy Mater.</i>	2021	3
TiO ₂ /ZnIn ₂ S ₄ /Zn _{0.6} Ca _{0.4} In ₂ S ₄	1.07 mA/cm ²		<i>Surf. Interfaces</i>	2021	4
ZnIn ₂ S ₄ -TS	0.95 mA/cm ²		<i>Adv. Energy Mater.</i>	2022	5
0.3-ZnIn ₂ S ₄ /TiO ₂	0.68 mA/cm ²		<i>J. Colloid Interface Sci.</i>	2023	6
ZnIn ₂ S ₄ /Cu ₂ S/NiFe-LDH	1.56 mA/cm ²		<i>Chem. Eng. J.</i>	2023	7
FO/ZnIn ₂ S ₄	1.88 mA/cm ²		<i>Angew. Chem. Int. Ed</i>	2024	8
ZnIn ₂ S ₄ -Sv-2h	2.18 mA/cm ²		<i>This work</i>	2024	

Table S2. Electrochemical impedance spectra of different samples under light conditions.

Sample	ZIS	ZIS-Sv-2h	ZIS-Sv-4h
$R_s / (\Omega)$	29.60	30.80	31.80
$R_{ct} / (K\Omega)$	4.60	1.32	2.62

Table S3. Electrochemical impedance of different samples under dark conditions.

Sample	ZIS	ZIS-Sv-2h	ZIS-Sv-4h
$R_s / (\Omega)$	42.20	40.70	39.40
$R_{ct} / (K\Omega)$	20.20	18.30	14.60

Table S4. Summary of recent significant progress of ZIS-based photoanodes for urea oxidation.

Photoanodes	Photocurrent		Journal	Year	Ref
	at 1.23 V vs. RHE				
SnO₂@BiVO₄/Co-Pi	3.44	mA/cm ²	<i>J. Mater. Chem. A</i>	2019	9
NiFeOOH/BVO	4.00	mA/cm ²	<i>Chem. Eng. J.</i>	2021	10
Fe₂O₃/Ni_{SP}	0.35	mA/cm ²	<i>Electrochim. Acta</i>	2023	11
ZnIn₂S₄-P₅	4.13	mA/cm ²	<i>Separations</i>	2024	12
ZnIn₂S₄-Sv-2h	4.60	mA/cm ²	<i>This work</i>	2024	

Table S5. Electrochemical impedance of different samples under light conditions.

Sample	ZIS	ZIS-Sv-2h	ZIS-Sv-4h
$R_s / (\Omega)$	47.30	42.70	36.80
$R_{ct} / (K\Omega)$	4.39	0.87	1.15

S 3.2 Reference

- 1 L. Xu, M. Li, F. Zhao, J. Quan, X. Ning, P. Chen, Z. An and X. Chen, *Appl. Catal., B*, 2024, **359**, 124503.
- 2 M. Zhou, Z. Liu, Q. Song, X. Li, B. Chen and Z. Liu, *Appl. Catal., B Environ.*, 2019, **244**, 188-196.
- 3 W. Xu, W. Tian, L. Meng, F. Cao and L. Li, *Adv. Energy Mater.*, 2021, **11**, 2003500.
- 4 X. Shi, C. Dai, X. Wang, P. Yang, L. Zheng, Z. Zhao and H. Zheng, *Surf. Interfaces*. 2021, **26**, 101323.
- 5 S. Li, L. Meng, W. Tian and L. Li, *Adv. Energy Mater.*, 2022, **12**, 2200629.
- 6 X. Zhao, N. Xi, W. Zhang, C. Cui, X. Su, X. Wang, X. Yu, H. Liu and Y. Sang, *J. Colloid Interface Sci.*, 2023, **650**, 1983-1992.
- 7 Z. Hao, R. Wang, L. Zhang, H. Sheng, Y. Li, B. Dong and L. Cao, *Chem. Eng. J.*, 2023, **468**, 143568.
- 8 S. Zhang, P. Du, H. Xiao, Z. Wang, R. Zhang, W. Luo, J. An, Y. Gao and B. Lu, *Angew. Chem. Int. Ed.*, 2024, **63**, e202315763.
- 9 J. Liu, J. Li, M. Shao and M. Wei, *J. Mater. Chem. A*, 2019, **7**, 6327-6336.
- 10 M. Sun, C. Yuan, R. T. Gao, R. Zhang, X. Liu, T. Nakajima, X. Zhang, Y. Su and L. Wang, *Chem. Eng. J.*, 2021, **426**, 131062.
- 11 L. Rebiai, D. Muller-Bouvet, R. Benyahia, E. Torralba, M. L. Viveros, V. Rocher, S. Azimi, C. Cachet-Vivier and S. Bastide, *Electrochim. Acta*, 2023, **438**, 141516.
- 12 J. Sun, L. Tang, C. Li, J. Quan, L. Xu, X. Ning, P. Chen, Q. Weng, Z. An and X. Chen, *Separations*, 2024, **11**, 268.